Principal Component Analysis of the Summertime Winds over the Gulf of California: A Gulf Surge Index

SIMONA BORDONI AND BJORN STEVENS

Department of Atmospheric and Oceanic Sciences, University of California, Los Angeles, Los Angeles, California

(Manuscript received 29 July 2005, in final form 21 February 2006)

ABSTRACT

A principal component analysis of the summertime near-surface Quick Scatterometer (QuikSCAT) winds is used to identify the leading mode of synoptic-scale variability of the low-level flow along the Gulf of California during the North American monsoon season. A gulf surge mode emerges from this analysis as the leading EOF, with the corresponding principal component time series interpretable as an objective index for gulf surge occurrence. This index is used as a reference time series for regression analysis and compositing meteorological fields of interest, to explore the relationship between gulf surges and precipitation over the core and marginal regions of the monsoon, as well as the manifestation of these transient events in the large-scale circulation. It is found that, although seemingly mesoscale features confined over the Gulf of California, gulf surges are intimately linked to patterns of large-scale variability of the eastern Pacific ITCZ and greatly contribute to the definition of the northward extent of the monsoonal rains.

1. Introduction

The southwestern (SW) United States, and Arizona in particular, experience a pronounced increase in rainfall from an extremely dry June to a rainy July, with summer rains usually lasting until mid-September after which a drier regime is reestablished over the region. The rapid onset of summer rains over Arizona is accompanied by a sudden shift and rearrangement of the hemispheric circulation, manifest in the northward and westward displacement of the two subtropical highs and the establishment of the midlevel anticyclone over northwestern Mexico. Consideration of this sequence of synoptic events, which causes the prevailing midlevel winds to shift from dry westerlies from the Pacific Ocean to moist southeasterlies, and the precipitation patterns over the arid Southwest led many early researchers to identify the Gulf of Mexico as the unique moisture source for the summer rains in this region (Bryson and Lowry 1955; Green and Sellers 1964; Reitan 1957; Hastings and Turner 1965). Only later, as it became increasingly recognized that the precipitation over the SW United States is but the northernmost extremity of a much more pronounced phenomenon centered over northwestern Mexico (Douglas et al. 1993) and now referred to as the North American monsoon (NAM; Adams and Comrie 1997), did the notion of the Gulf of California (GoC) as a possible moisture source for the monsoonal convection start appearing prominently in the literature.

In the early 1990s, dedicated field studies as part of the Southwest Area Monsoon Project (SWAMP) were conducted to provide a better documentation of the monsoonal circulation with a special focus over the core monsoon region, by means of special radiosondes, pilot balloons, and National Oceanic and Atmospheric Administration (NOAA) WP-3D aircraft flights (Meitin et al. 1999). Mean streamlines of the lower-tropospheric flow derived from these mesoscale observations suggest the existence of a persistent southerly low-level jet along the GoC during the summer season, capable of advecting northward large amounts of water vapor. Recent modeling and diagnostic studies support the view of this low-level jet over the GoC as the primary mode of low-level moisture transport from the tropical Pacific/GoC into the elevated terrain over northwestern Mexico and into the SW United States (Schmitz and Mullen 1996; Berbery 2001). Seemingly suggestive of the role that the GoC may be playing in the development and extent of the monsoonal rains is the finding

Corresponding author address: Simona Bordoni, Dept. of Atmospheric and Oceanic Sciences, University of California, Los Angeles, Box 951565, 405 Hilgard Ave., Los Angeles, CA 90095-1565.
E-mail: bordoni@atmos.ucla.edu

that for the monsoon to be successfully simulated exceptionally warm waters have to be present in the gulf (Stensrud et al. 1995). A recent empirical study by Mitchell et al. (2002) further argues that the northward propagation of rainfall and convection may be related to the northward propagation of the 29°C SST isotherm into the GoC.

While the general understanding of the NAM has greatly improved in the last decade thanks to extensive research, there are a number of important questions that still need conclusive answers. One, which motivates this work, is how the contribution to the total moisture transport by the time-mean circulation and the transient eddies is partitioned. The episodic nature of the summer thunderstorms over the marginal regions of the NAM has in fact been associated with the anomalous northward influx of gulf moisture by transient events, operationally known as gulf surges. Gulf surges along the GoC, initially described in the early 1970s (Hales 1972), are northward surges of relatively cool, moist maritime air from the tropical Pacific into the southwestern desert region, which occur every summer during the NAM season. Because of the sparsity of lower-tropospheric observations over the GoC and differing definitions among authors, our understanding of the gulf surge phenomenon is still in its infancy. The relatively few works that have described the structure and frequency of surges and explored their relationship with precipitation have been based on gulf surge identification methods that rely on observations from a single station (Douglas and Leal 2003; Higgins et al. 2004).

Bordoni et al. (2004) have used 5 yr of 10-m ocean wind measurements by the Quick Scatterometer (QuikSCAT) to characterize the changes in the low-level circulation associated with the NAM. Their analysis shows that the wind field over the entire GoC undergoes a well-defined monsoonal reversal from northwesterly flow during the winter to south-southeasterly flow during the summer, thus confirming that the low-level jet sampled during the SWAMP campaign is representative of the summertime mean circulation and an integral component of the monsoon system itself. In the heart of the monsoon season, the time-mean flow is found to be composed of periods of enhanced southerly winds associated with gulf surges. The histogram of the summertime GoC winds, which features a bimodal distribution, identifies these transients as events sampled from a distribution distinct from the background flow, supporting the view of gulf surges as a distinct dynamical mode capable of providing anomalous moisture transport into the core and marginal regions of the monsoon.

The results in Bordoni et al. (2004), which appear to reinforce the role that the GoC and its topography play in the development of the monsoon, raise further questions as to what extent the onset, subsequent evolution, and the northward extension of the summertime rainfall can be related to the evolution of the GoC low-level winds and the strong seasonal warming in its waters. Can the moisture transport provided by the time-mean circulation over the GoC explain the overall distribution and northward extension of precipitation in the NAM region, as results from the diagnostic study by Schmitz and Mullen (1996) suggest? If not, are gulf surges, so remarkably evident in the QuikSCAT data, a thread through which some of the mysteries of the monsoon as a whole may be unraveled? To answer these questions, we perform an empirical orthogonal function (EOF) analysis of the daily June–September QuikSCAT winds for six summers (1999–2004) to objectively determine the leading modes of variability in the low-level winds over the GoC on the synoptic time scales. A "gulf surge mode," which appears as a robust, spatially coherent structure in the near-surface winds, emerges from this analysis as the leading EOF. This allows us to interpret the corresponding standardized principal component (PC) time series, which proves to be nearly identical apart from a scaling factor to the domain-averaged wind anomalies time series, as an objective index for gulf surge occurrence. This index is then used as a reference time series for regression analysis and compositing meteorological fields of interest. While our main focus is on exploring how gulf surges modulate the precipitation in the core and marginal regions of the monsoon, we also document how the atmospheric circulation varies in association with the surge index and how these results compare with previous work based on more traditional definitions of gulf surge events (Higgins et al. 2004).

After a brief overview of the datasets and the methodology used in this study in section 2, in section 3 we present the gulf surge index based on the EOF analysis of the summertime QuikSCAT winds and we establish its relation to gulf surge events. Section 4 explores the relationship between gulf surges and precipitation, and in section 5 we examine the relationship between gulf surges and tropical disturbances. A discussion of our results is presented in section 6: in section 6a we explore how and to what extent the results shown in sections 3, 4, and 5, mostly based on the National Centers for Environmental Prediction–National Center for Atmospheric Research (NCEP–NCAR) reanalysis fields, differ from results based on the higher spatial resolution but more temporally limited European Centre for Medium-Range Weather Forecasts (ECMWF) 40-yr Re-

Analysis (ERA-40), and in section 6b we discuss how our gulf surge index differs and compares to other indices already existing in the literature. A summary of our major findings follows in section 7.

2. Data and methodology

The basic dataset used in this study consists of QuikSCAT winds, obtained from the National Aeronautics and Space Administration–Jet Propulsion Laboratory (NASA–JPL) level 3 daily, gridded wind vectors with a horizontal grid spacing of 0.25°. In situ studies (Ebuchi et al. 2002; Pickett et al. 2003; Bourassa et al. 2003) have shown that QuikSCAT wind retrievals are accurate to better than the mission-stated accuracy of 2 m s^{-1} in speed and 20° in direction. For each day, both ascending and descending pass measurements are provided. Typically these correspond to gulf-crossing times near 0500 and 1700 LST, respectively. The exact crossing time and the degree of coverage vary with a 4-day cycle, during which periods of "bursts" of closely spaced samples are separated by longer temporal gaps (Schlax et al. 2001). Over the GoC, sampling intervals are never longer than 24 h; thus, measurements are sufficiently frequent to allow for the resolution of synoptic-scale variability in the low-level circulation.

To examine the principal mode of the subseasonal variability in the summertime low-level circulation along the GoC, the available ascending and descending measurements are averaged to construct daily time series of zonal and meridional wind anomalies during the NH summer (June–September). The seasonal cycle and the seasonal means for each individual summer have both been removed in order to isolate processes that occur on the intraseasonal time scale, which is the main focus of this study, from processes that occur on interannual time scales. The principal component analysis is based on the temporal unstandardized covariance matrix of the alongshore wind anomalies, that is, the component of the wind parallel to the GoC axis and defined positive for northward flow, in an oceanic strip along and south of the GoC (from 20° to 32°N). This relatively small domain has been chosen to isolate synoptic-scale variability associated with gulf surges, known to be a mesoscale phenomenon that mostly affects the GoC, from synoptic-scale variability in the larger-scale flow over the northeast Pacific Ocean. Because of the low latitude and limited meridional extent of the domain, cosine weighting was not considered necessary. Rather than displaying the actual EOFs, we regress the daily alongshore winds upon the standardized PC time series and we display the resulting covariance coefficients. Regression maps of other meteorological fields upon the leading PC have been constructed in a similar way. Because the standardized PC time series is dimensionless, these regression maps have the same units as the anomaly field itself and their amplitudes correspond to anomaly values in that field that occur in association with a one standard deviation anomaly in the independent variable, that is, the index time series. The statistical significance of all regressions has been assessed using a t statistic in which the effective sample size is reduced to account for the temporal correlation in the data following the procedure of Livezey and Chen (1983). While the results shown here represent the most preferred patterns of gulf surge events, there is a large variability between individual events, which is not explored here and requires further investigation.

The precipitation dataset is the Global Precipitation Climatology Project (GPCP) One-Degree Daily Precipitation Dataset (1DD), which provides globally complete daily estimates of precipitation (mm day^{-1}) on a $1° \times 1°$ latitude–longitude grid from currently available observational data, from January 1997 through the present (Huffman et al. 2001). The remaining data were obtained from both the NCEP–NCAR reanalysis (Kalnay et al. 1996) and the ERA-40 dataset (Uppala et al. 2005). The NCEP–NCAR reanalysis is based on a T62, 28-level model and provides a global dataset on a 2.5° horizontal grid. The ERA-40 reanalysis, based on the ECMWF Integrated Forecasting System run with a T159 truncation and 60 vertical levels, provides fields on a much finer grid (~1.1°), but has the disadvantage of being available only up to August 2002, thus overlapping with the QuikSCAT data during only four summer seasons.

3. A gulf surge index

When investigating the time and space scales of the variability of the NAM precipitation, and the associated large-scale circulation, it would appear natural to define appropriate indices that are based on the precipitation field itself, as previously done by a number of studies. By means of an EOF analysis of monthly mean precipitation anomalies, Yu and Wallace (2000) have, for instance, examined the principal mode of the interannual variability of the NAM in an extended domain (5°–35°N, 125°–80°W), encompassing not only the continental regions with pronounced summertime precipitation maxima, but also the adjacent ocean waters to the south of Mexico and Central America. Higgins and Shi (2001) have extended this analysis to more carefully distinguish the interannual and the intraseasonal modes of variability of the monsoon in the same domain, using seasonal, monthly, and pentad-mean precipitation data.

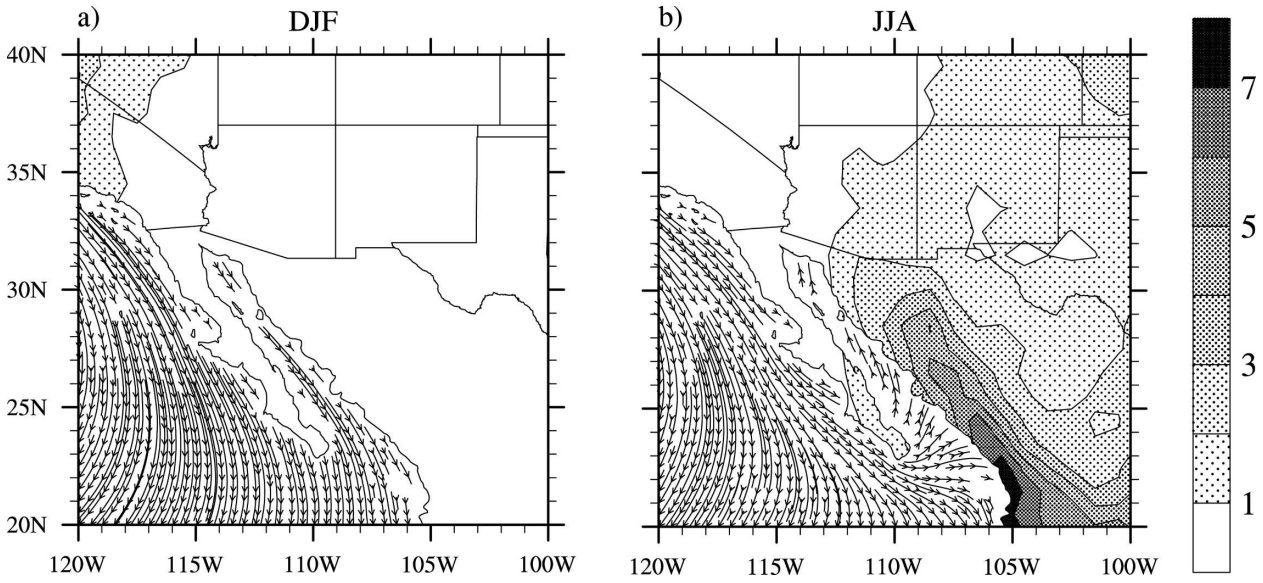

FIG. 1. Mean streamlines of the 10-m winds over the GoC as derived from QuikSCAT observations of (a) December–February (DJF) and (b) June–August (JJA). Contours over land show the mean daily precipitation (mm day^{-1}) from the GPCP 1DD dataset.

They found that the leading PC from the summertime seasonal-mean data is associated with ENSO variability, while the leading PC from the pentad-mean data is associated with 30–60-day Madden–Julian oscillation (MJO). The application of such a methodology to daily, high-pass-filtered (so as to remove signals associated with the MJO) precipitation data, as an unambiguous method to isolate the variability in the NAM precipitation in the submonthly time scales, although seemingly straightforward, presents one major problem: the identification of an appropriate analysis domain. When using the extended domain of Yu and Wallace (2000), the leading PC accounts for only a small fraction of the total variance and, being poorly separated from the following few PCs, is not easily interpretable; for smaller domains, which do not include the oceanic ITCZ over the tropical eastern Pacific, the leading PCs are not robust to even small changes in the domain boundaries. For these reasons, we adopt a different tactic: rather than isolating the precipitation patterns that explain the largest fraction of the variance in the NAM region, and determining the synoptic conditions that produce such precipitation patterns, we define a dynamical index of the transient activity in the low-level winds along the GoC associated with gulf surges and we investigate what fraction of the total summertime precipitation these events account for.

As a reference, Fig. 1 shows the climatological December–February (Fig. 1a) and June–August (Fig. 1b) near-surface ocean winds in the oceanic monsoon region. The southerly flow that becomes established over the entire GoC appears as the distinctive feature of the summertime mean circulation, which is otherwise dominated by northerly flow around the Pacific subtropical high. The standardized daily time series (15 June–15 September) of the leading PC of the alongshore wind anomalies in the domain confined in an oceanic strip along and south of the GoC (from 20° to 32°N) is shown in Fig. 2. This time series accounts for ~50% of the variance and is well separated from the other eigenvalues as per the criterion of North et al. (1982). The correlation coefficient between this reference time series and the time series of the domain-averaged alongshore wind anomalies is 0.97, thus suggesting that the leading PC may be interpreted as a simple index for the variations from the summertime mean of the alongshore wind over the GoC as a whole. To ensure that our results do not depend on the specific scalar quantity chosen for the analysis, that is, the alongshore wind, the EOF analysis has been repeated on wind vectors using the real-vector method of Kaihatu et al. (1998): the leading PCs determined with the two methods are found to correlate at the 0.99 level. EOF analyses performed on larger domains also show that the leading PC is robust to changes in the domain size. As the domain of the analysis encompasses increasingly larger areas over the northeast Pacific Ocean, the leading PC time series accounts for a decreasingly smaller fraction of the total variance, but remains relatively unchanged.

The spatial pattern of the near-surface QuikSCAT winds regressed on the PC time series in the monsoon-

extended domain is shown in Fig. 3a. In its positive polarity, the reference time series is associated with a localized cyclonic anomaly to the southwest of the tip of Baja California. The flow around this circulation center provides anomalous westerly winds to its southern flank in the 10°–20°N belt and strong anomalous southeasterly winds south and along the GoC to its eastern flank. No significant anomalies are evident in the circulation over the Pacific Ocean north of 25°N. Figures 3b and 3c show the same regression pattern as in Fig. 3a, but are based on the ERA-40 and the NCEP–NCAR 10-m winds, respectively. Bordoni et al. (2004) have shown that the NCEP–NCAR reanalysis product, because of the inadequate resolution of the topography of the region, does not provide an accurate description of the summertime behavior of the low-level circulation over the GoC; in particular, in their Fig. 2 a comparison plot of the coastal strip average of the GoC June–September (JJAS) alongshore flow as derived from QuikSCAT and the NCEP–NCAR reanalysis shows that the NCEP–NCAR winds indicate northerly rather than southerly alongshore flow over the entire gulf.[1] A similar analysis based on the ERA-40 data shows in contrast a remarkable agreement between the reanalysis and the observed winds over the southern and central parts of the GoC, highlighting the capability of this reanalysis product to capture the seasonality of the low-level flow over the GoC and confirming the importance of resolving the GoC topography for realistically representing the NAM features. Despite its coarser spatial resolution and its lower performance over the NAM domain as compared with the ERA-40, NCEP–NCAR reanalysis proves however to be a valuable tool for our regression analysis: a comparison of Figs. 3a–c reveals that the regression pattern based on the NCEP–NCAR winds captures the main features of interest within the limits of the dataset horizontal grid spacing, which indicates that despite its limitation in describing the summertime mean circulation over the GoC, the NCEP–NCAR reanalysis captures well the anomalous fields associated with the leading PC. In addition, unlike the ERA-40, which is only available up to August 2002, it provides the notable advantage of covering the entire time span upon which our EOF analysis is based, thus allowing us to construct more robust covariance maps. Confronted with the choice between the higher-resolution, but temporally limited, ERA-40 and the coarser-resolution, but temporally extended, NCEP–NCAR product, we therefore select the latter as the basis of the regression analysis shown in the following sections. The question of how and to what extent our results differ when based on the ERA-40 reanalysis is explored in section 6.

The time evolution of the low-level wind anomalies associated with the leading EOF can be characterized by constructing lagged regressions of the near-surface QuikSCAT winds on the reference time series. Such regressions are shown from day −3 to day +2 in Fig. 4. At early lags, westerly anomalies in the region of climatological easterly flow from 10° to 20°N appear as the strongest signal. At day −2 anomalous northerly winds span the GoC, while evidence of a weak cyclonic circulation center is found at ~20°N on the west coast of mainland Mexico. In the following days, this cyclonic anomaly becomes more coherent and propagates northwestward, moving to the southwest of the tip of Baja California at day 0; at this time, the southeasterly anomalies, previously confined at lower latitudes, have propagated northward into the GoC and cover its entire length. Propagation of the northward flow is still evident at day +1. At day +2, as the cyclonic center keeps moving northwestward, wind anomalies over the GoC weaken and lose coherence.

Although differing definitions of gulf surges exist in the literature, qualitatively they all share the idea that a gulf surge can be defined as the development of a strong southerly or southeasterly flow along the GoC. Accompanying the wind shift one often finds a rise in dewpoint, a drop in temperature, and a general increase in low clouds and convective activity. The strong anomalous alongshore wind that is found over the GoC

[1] One might wonder if and to what extent QuikSCAT and NCEP–NCAR provide independent wind data, given that the wind field from the NCEP Numerical Weather Product (NWP) model is used to initialize the median filter algorithm that removes the direction ambiguity in the QuikSCAT measurements. In fact, scatterometer wind retrievals generally yield multiple solutions, or ambiguities, at each wind vector cell, which come about from the sinusoidal relationship between the measured radar-backscattered power and the angle between the radar look direction and the wind direction. Each ambiguity has an associated likelihood, but as there is no assurance that the most probable ambiguity is the correct choice, a spatial filter or ambiguity removal scheme has to be used to select from all possible ambiguities the wind solution closest to the true wind. In the scheme adopted by NASA to produce the QuikSCAT winds, the NWP is used to nudge the initial estimate of the wind field, then a modified point-wise median filter iteratively selects at each wind vector cell the ambiguity from all available solutions best matching the flow of the surrounding cells. The nudging technique therefore improves the overall ambiguity removal process in that it guarantees a fast convergence to the final solution in regions where the NCEP–NCAR first guess is close to the actual wind, without preventing the algorithm from converging to the true wind in all other regions, such as the GoC, where NCEP–NCAR is found to be inaccurate. More information about the L3 QuikSCAT winds can be found online (http://podaac.jpl.nasa.gov:2031/DATASET_DOCS/qscat_L3.html).

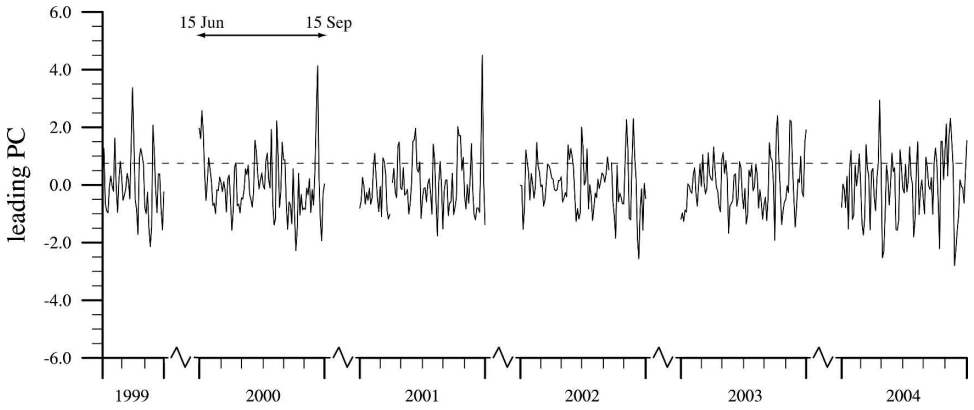

FIG. 2. Time series of the standardized leading PC of the daily alongshore wind anomalies over the GoC for JJAS 1999–2004. Note the discontinuity in the time (x) axis. We define values greater than 0.75 (indicated by the dashed line) to be surge events.

in association with the leading EOF therefore suggests that there may be a relationship between the principal mode of the synoptic-scale variability of the summertime low-level circulation and the onset of a gulf surge event. We explore this relationship further by constructing regression maps of sea level pressure (SLP), air temperature, and specific humidity time series from the NCEP–NCAR data on the leading PC to characterize the "average structure" of the reference time series. Superimposed on the winds, lagged regressions of the SLP are shown in Fig. 4. Consistently with the wind fields, the SLP anomalies show evidence of a northwestward migration. The elongated negative pressure anomaly that at day −2 is found over the GoC moves to the north or northwest at lesser lags, and is succeeded by ridging over the gulf and a developing low pressure system associated with the cyclonic circulation westsouthwest of Baja California. The evolution of the 925-hPa air temperature anomalies (Fig. 5) closely tracks the changes in SLP. Warmer-than-normal temperatures found over the GoC and the SW United States at negative lags are replaced by colder-than-normal temperatures as the high pressure tongue propagates into the region. Lagged regressions of the 925-hPa specific humidity in Fig. 6 show that these abrupt changes in low-level winds, SLP, and air temperature are accompanied by northward-propagating, positive specific humidity anomalies: at negative lags, drier-than-normal conditions are found over the entire core monsoon region, including the SW United States. At day −1, enhanced moisture appears in association with the southerly flow confined just south of the entrance of the GoC. At day 0, as the specific humidity anomalies have intensified and propagated northward, a sharp humidity boundary is found over the Midriff Islands located in the central GoC at around 30°N,

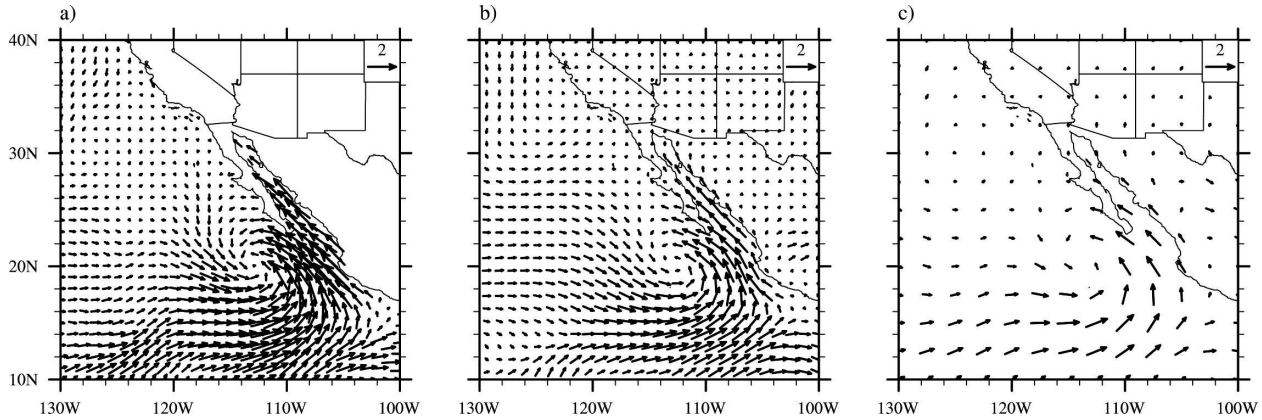

FIG. 3. Regression patterns of daily 10-m (a) QuikSCAT, (b) ERA-40, and (c) NCEP–NCAR winds on the reference time series shown in Fig. 2.

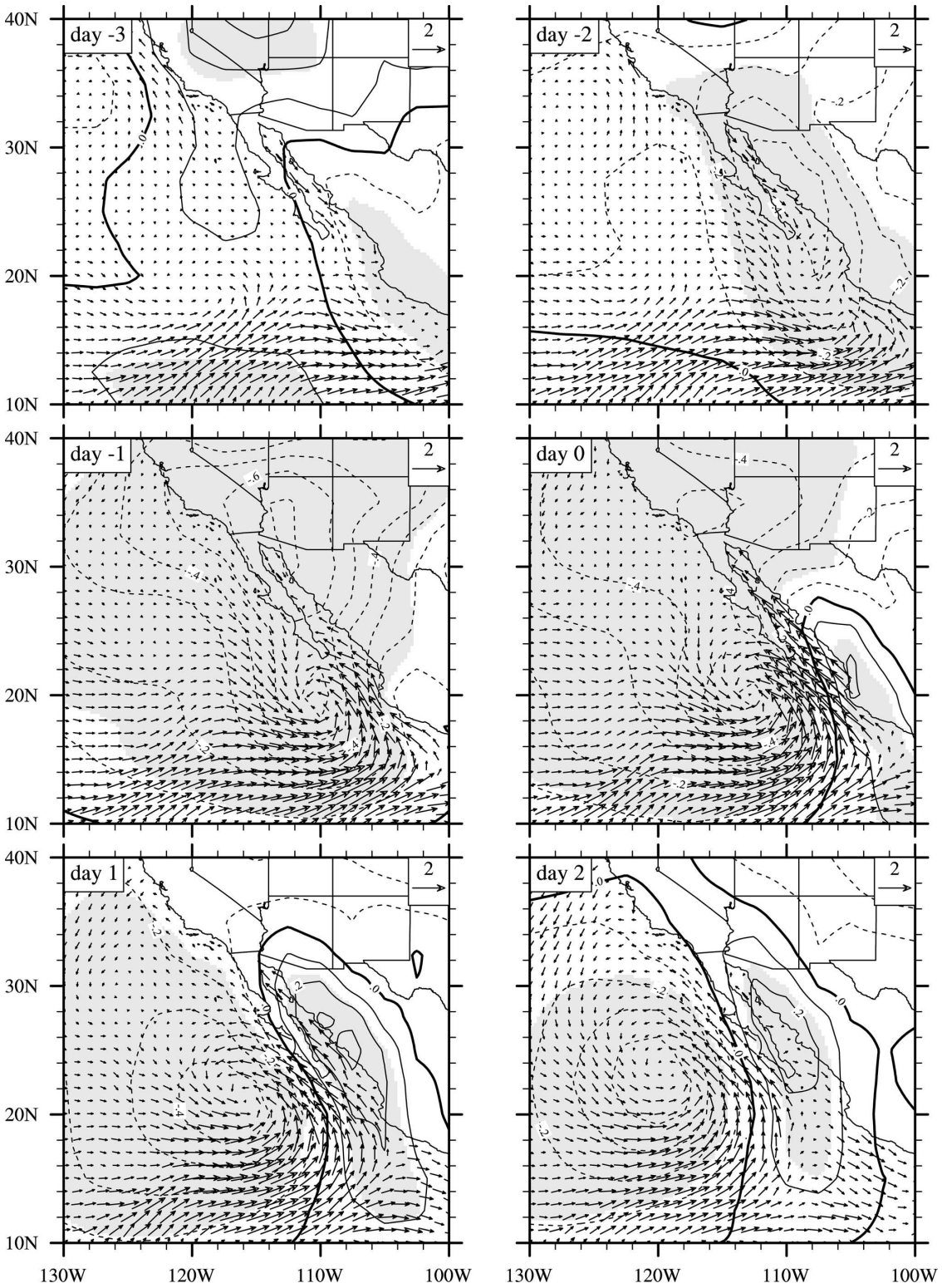

FIG. 4. Lagged regressions from day −3 to day +2 of the QuikSCAT low-level wind vectors and the NCEP–NCAR SLP (contours) onto the leading PC. The contour interval is 0.1 hPa. Negative anomalies are dashed and the zero line thickened. Shading indicates regions where anomalies are statistically significant at the 95% level.

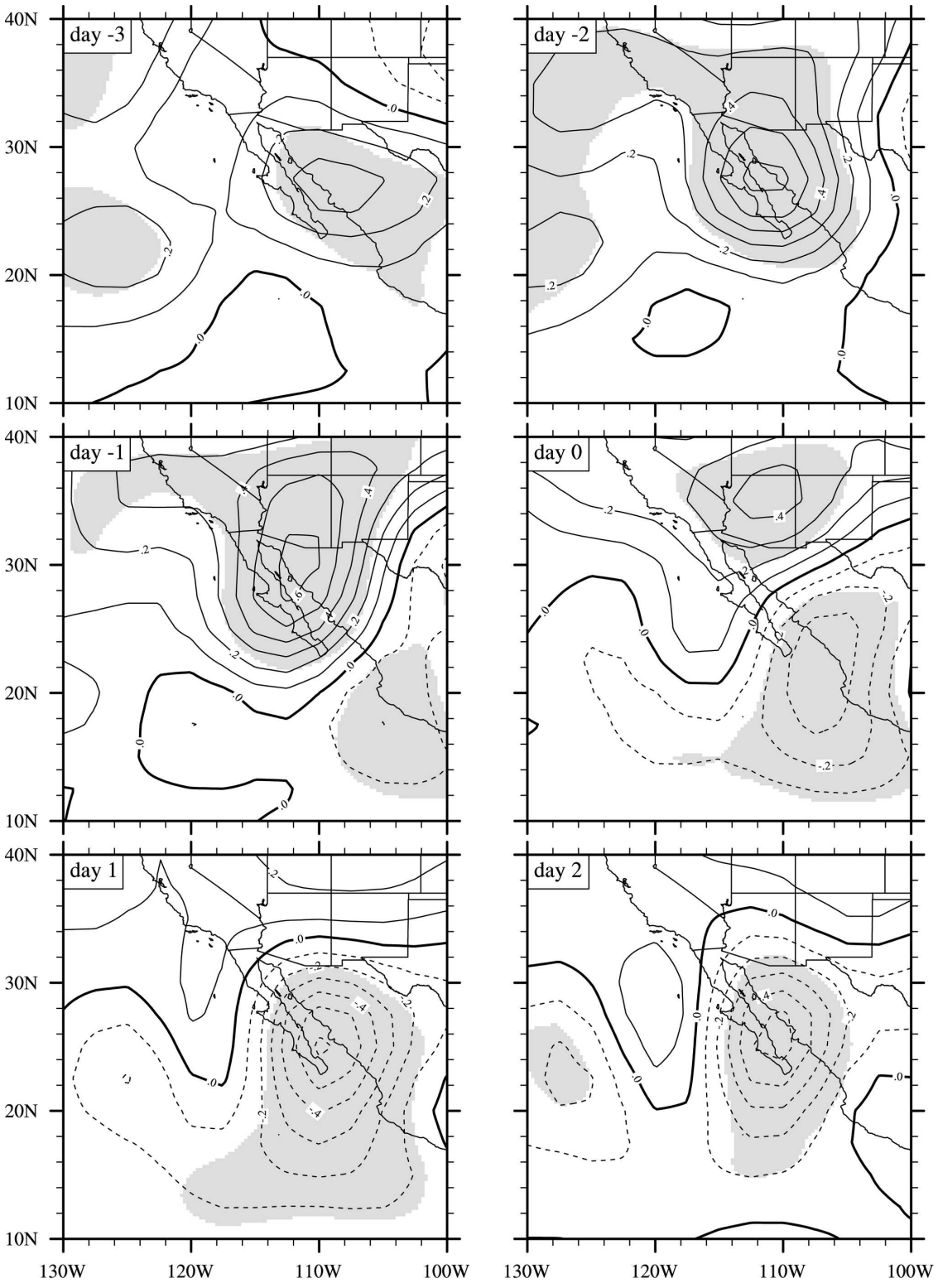

FIG. 5. Lagged regressions from day −3 to day +2 of the NCEP–NCAR 925-hPa air temperature onto the leading PC. The contour interval is 0.1°C. Negative anomalies are dashed and the zero line thickened. Shading indicates regions where anomalies are statistically significant at the 95% level.

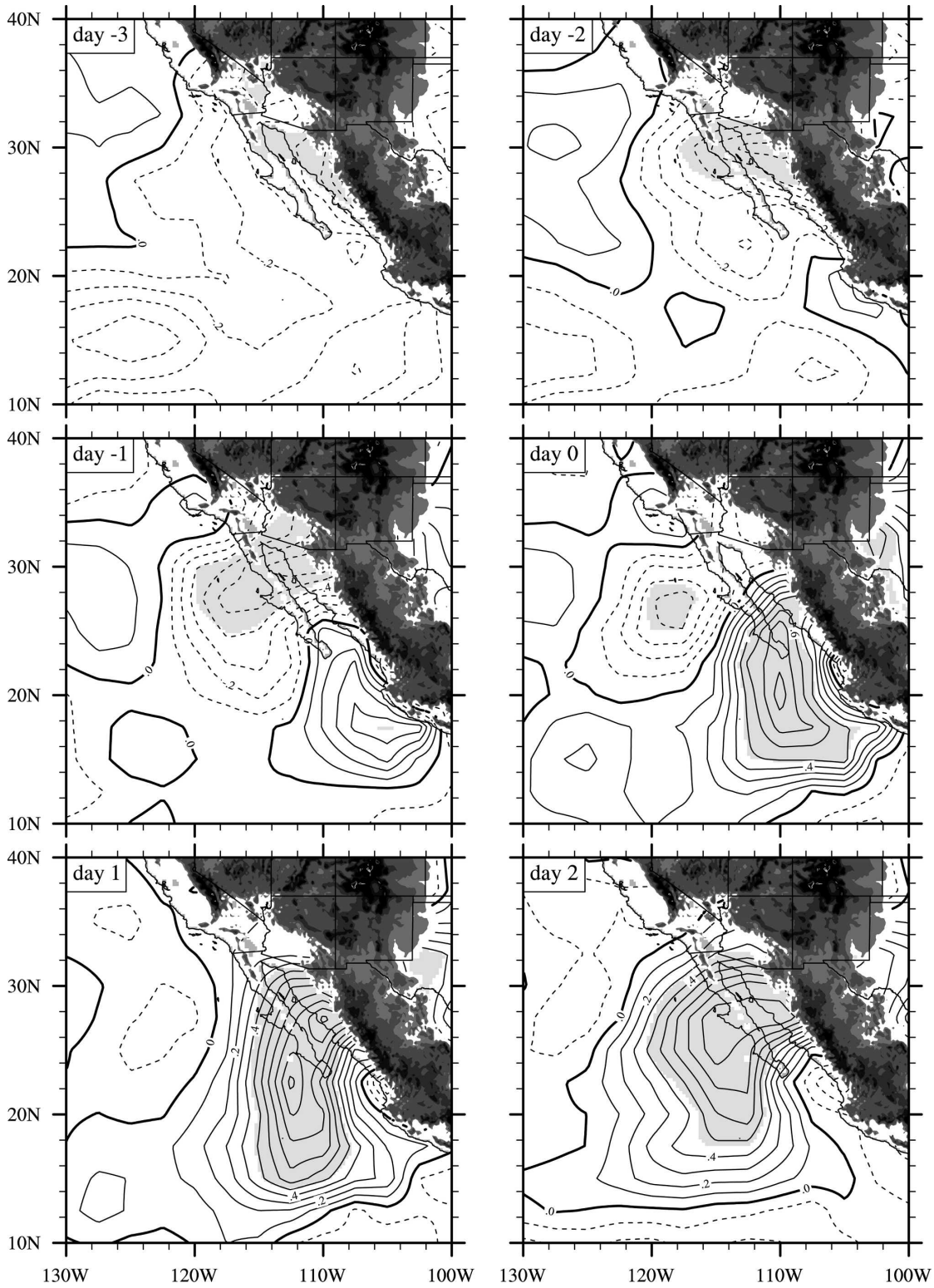

FIG. 6. Lagged regressions from day −3 to day +2 of the NCEP–NCAR 925-hPa specific humidity onto the leading PC. The contour interval is 0.1 g kg^{-1}. Negative anomalies are dashed and the zero line thickened. Shading indicates regions where anomalies are statistically significant at the 95% level. Areas with topography (in grayscale contours) above the 925-hPa level have been masked out.

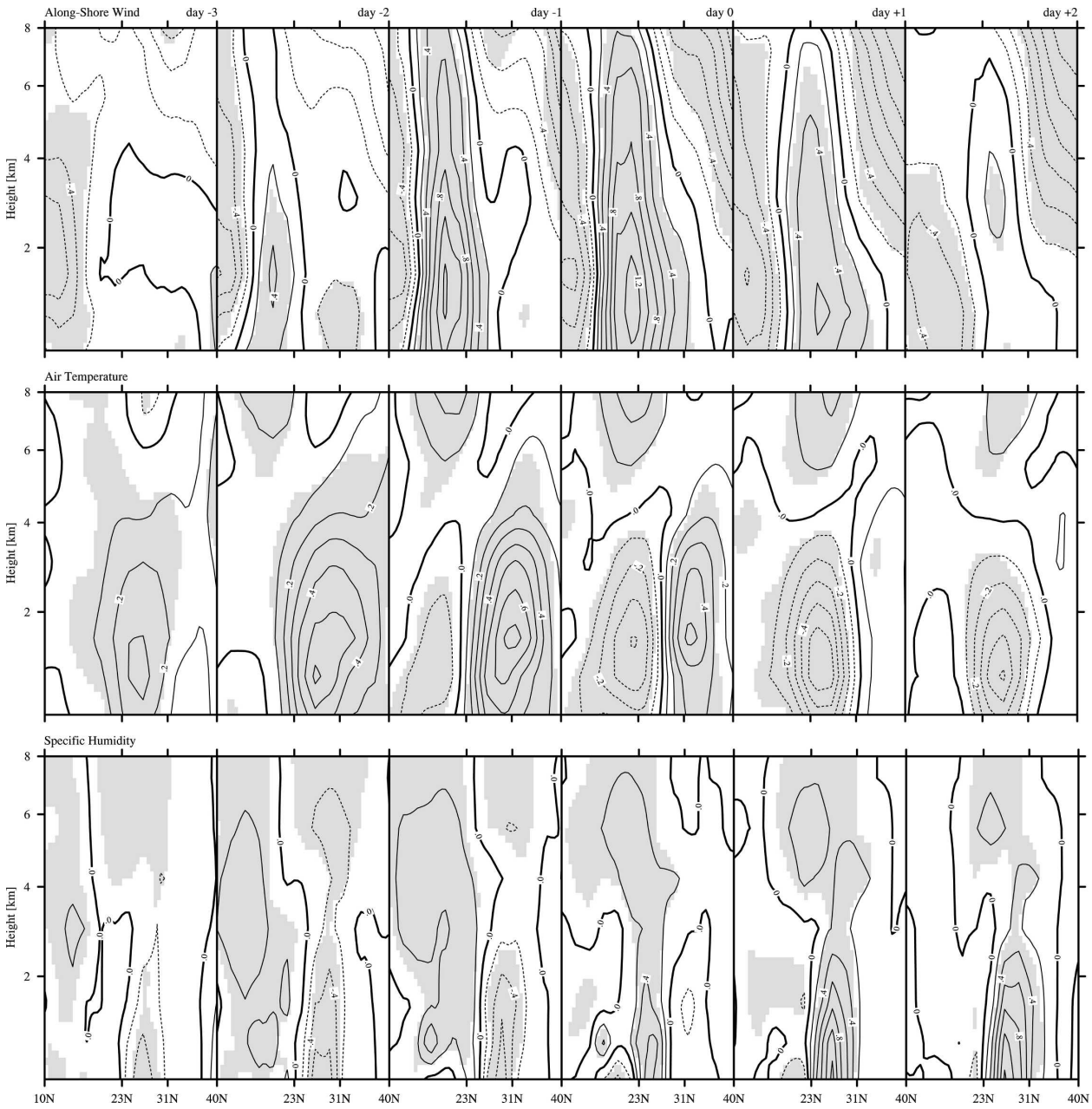

FIG. 7. Vertical cross sections of the (top) alongshore wind, (center) air temperature, and (bottom) specific humidity regressed on the leading PC along a transect across the GoC from 10° to 40°N. The contour interval is 0.2 m s^{-1} for the alongshore wind, 0.1°C for the air temperature, and 0.2 g kg^{-1} for the specific humidity. Negative anomalies are dashed and the zero lines thickened. Shading indicates regions where anomalies are statistically significant at the 95% level. Tick marks at 23° and 31°N show the southern and northern end of the GoC, respectively, along the selected transect.

while at day +1 such a boundary has propagated northward into Arizona and New Mexico.

Vertical cross sections of the alongshore wind, air temperature, and specific humidity regressed on the leading PC at different lags along a transect across the GoC from 10° to 40°N are shown in Fig. 7. The selection of this relatively large span for the vertical cross sections is motivated by the regression maps of Figs. 4–6, in which field anomalies do not appear to be localized over the GoC, but extend over a wider region. The largest positive alongshore wind anomalies (Fig. 7, top), which are not confined to a shallow layer close to the surface but extend beyond 8 km with a maximum at around 1 km from the surface, are found at day −1 and

day 0 south of and along the GoC. The abrupt onset of the enhanced alongshore wind at this time is accompanied by a shift from positive to negative air temperature anomalies (Fig. 7, center) and from negative to positive specific humidity anomalies (Fig. 7, bottom) over the GoC. While specific humidity anomalies feature maxima close to the surface, the air temperature anomalies maximize at higher heights. Interestingly, we find that the warm anomaly prior to day 0 substantially exceeds that of the cold anomaly at following lags.

Given that a wind shift from northerly, or weak southerly, to strong southerly flow; an increase in moisture; and a drop in temperature are all believed to be common characteristics of gulf surges, these results suggest that the leading EOF of the GoC alongshore winds can be interpreted as a gulf surge mode and motivate our definition of the associated PC time series as a "gulf surge index." In light of this interpretation of the reference time series, the regression patterns shown here can therefore be thought of as the preferred anomaly patterns associated with gulf surge events and can be compared to composites of the surge structure and evolution presented in previous modeling and observational studies (Anderson et al. 2000; Douglas and Leal 2003). In particular, the general agreement with the composite structure of 38 surge passages at Empalme in Douglas and Leal (2003), based on 9 yr of radiosonde observations and NCEP–NCAR reanalyses, is remarkable. Our results, however, seem to indicate that gulf surge signatures are more vertically extended than previously thought: with the strongest wind, temperature, and humidity anomalies confined to the lower troposphere, weaker but still significant anomalies are also found at higher elevations. While these could arguably be artifacts of the poor representation of the state of the troposphere over the GoC by the NCEP–NCAR reanalysis, as we shall see in section 6 they are also evident, and even more pronounced, in vertical cross sections based on the ERA-40 data.

4. Surges and precipitation

While early works suggest a connection between surges and severe thunderstorms over the marginal regions of the monsoon, the relationship between gulf surges and the amount of rainfall over the GoC and the surrounding areas has only begun to be investigated and quantified by recent studies (Douglas and Leal 2003; Higgins et al. 2004; Gochis et al. 2004). The definition of a gulf surge index, based on the daily variability of the alongshore winds over the GoC, allows us to explore in detail this relationship. We begin by constructing lagged regressions of precipitation (mm day^{-1}), as derived from the GPCP 1DD on the surge index, which are shown in Fig. 8. In the days preceding the onset, conditions are found to be drier than normal everywhere in the core monsoon region and wetter than normal over the tropical Pacific south of the GoC entrance, where the analysis in Fig. 4 shows converging anomalous westerly flow. Positive precipitation anomalies are also found over the east coast of Mexico and the Gulf of Mexico. At the onset (day 0), the positive anomalies have propagated northward into the GoC and span the entire coast of northwestern Mexico. The northward migration of the positive precipitation anomalies continues after the onset, when wetter-than-normal conditions are found over the SW United States and drier conditions are reestablished to the south of the GoC. The regressions maps shown in Fig. 8 share important common features with the ones in Figs. 4–6: the precipitation anomalies, like all other anomalies, do not appear to be confined to the GoC but extend far south of its entrance and show evidence of northwestward progression along the west coast of mainland Mexico from the tropical Pacific to the SW United States, thus suggesting a relationship between gulf surges and tropical disturbances. This relationship will become more apparent in the analysis presented in the next section. In addition, the regression maps in Fig. 8 clearly demonstrate that GoC surges are associated with considerable changes in the precipitation pattern over northwestern Mexico and the SW United States, thus suggesting that a large fraction of the summertime precipitation in this area may be attributable to low-level moisture inflow by transients.

To give a quantitative estimate of the contribution to the total summertime precipitation made by gulf surges, we identify the onset of individual surge events with days in which the index time series equals or exceeds 0.75, that is, 75% of its standard deviation, and we attribute to a surge event the precipitation falling in the monsoon area within 4 days after the surge onset. Of course the strict adherence to such a threshold would not be possible operationally, but the general association between surges and strong positive alongshore wind anomalies could provide a simple criterion for real-time identification of gulf surges. In this way, we identify 59 gulf surge events for our entire analysis period (15 June–15 September 1999–2004), with an average frequency of three to four surges per month in agreement with previous studies (Fuller and Stensrud 2000; Douglas and Leal 2003; Higgins et al. 2004), and we partition the summer days in surge and nonsurge days as explained above. As shown in Fig. 9, it is found that the surge events, which correspond to ~46% of the total number of days, explain a fraction of the summer-

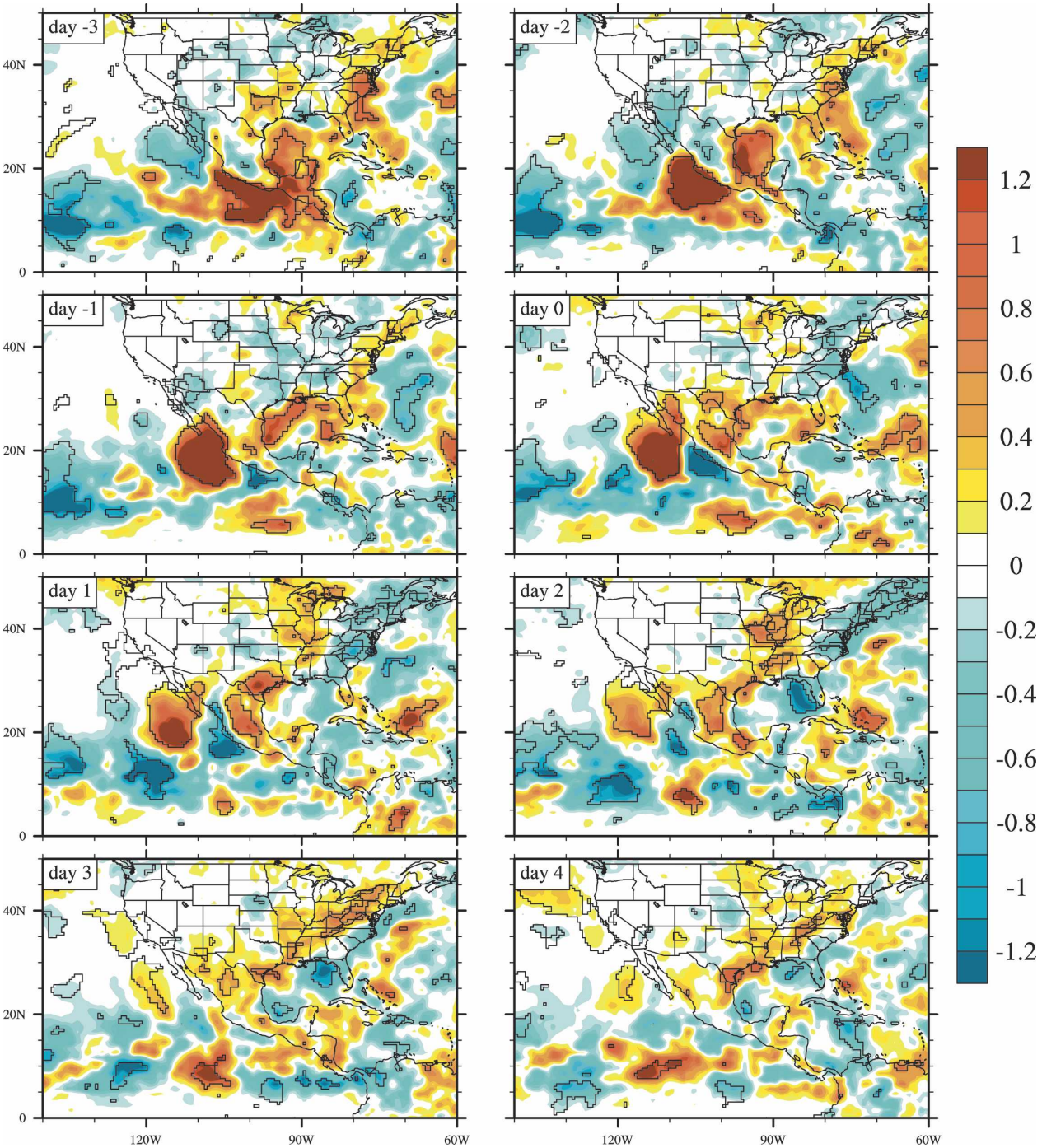

FIG. 8. Lagged regressions from day −3 to day +4 of the GPCP 1DD precipitation (mm day^{-1}) onto the gulf surge index. Solid contours delimit regions where anomalies are statistically significant at the 95% level.

time precipitation that is equal to or larger than 50% over the entire monsoon domain. The influence of gulf surges appears to be the greatest in the coastal areas adjacent to the GoC and over Arizona, where the contribution to the total rainfall by surge events exceeds 70%. Daily rain rates computed for surge and nonsurge days shown in Fig. 10 confirm that the mean daily precipitation falling over these areas during nonsurge days is almost negligible, being everywhere less that 1 mm day^{-1}. Over the core of the monsoon and the higher-elevation regions of the Sierra Madre Occidental, where the diurnal cycle and the orographic forcing are

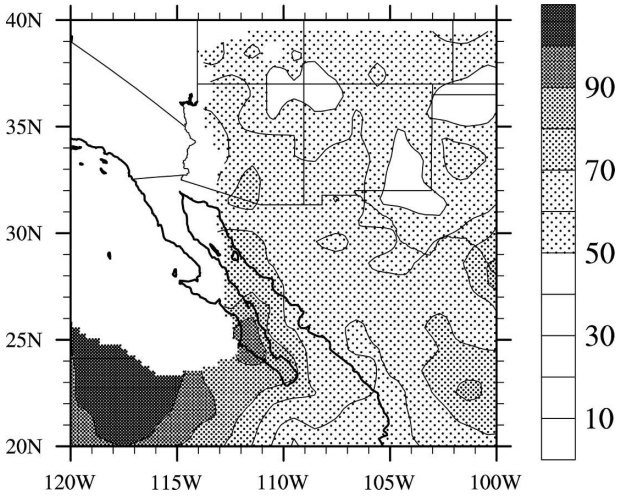

FIG. 9. Percentage of total summertime rainfall during surge days. Areas where the mean climatological daily precipitation is less that 0.5 mm day^{-1} have been masked.

believed to be the dominant dynamical mechanisms for convection initiation, surge and nonsurge days show comparable values of daily rain rates. Similar patterns, based on surge events occurring during one summer, have been found in Berbery and Fox-Rabinovitz (2003) and Gochis et al. (2004).

While the threshold in the gulf surge index chosen to identify individual surge events is somewhat arbitrary, results with larger and smaller values of the threshold do not differ qualitatively from the ones presented in Figs. 9 and 10. These results are summarized in Table 1, where we present the ratio of the area mean percentage of the summertime precipitation falling during surge days to the percentage of the total summer days that those surge days represent, for different values of the index threshold in three boxes: Arizona (31°–34°N, 112°–109°W), New Mexico (31°–34°N, 109°–103°W), and the Sonora coastal region (26°–31°N, 112°–109°W). Independently of the chosen threshold, in each of the three boxes the fraction of the summertime precipitation occurring during surge days is larger than what one would expect if surge and nonsurge days had comparable daily rain rates. For the coastal areas along the eastern side of the GoC and Arizona, this appears to be particularly true for higher values of the chosen threshold, thus revealing that stronger surges along the GoC are major contributors to summertime convective episodes in these regions. The decaying influence of gulf surges away from the GoC helps explain the smaller ratios, and evidence of no significant trend with higher thresholds, found over New Mexico, whose eastern portion appears to also be affected by factors unrelated to gulf surges.

It is worth emphasizing that the results shown here are based on an averaging procedure, which does not consider surge-to-surge variability. Consideration of such a variability would allow us to more precisely account for individual surge persistence and to exclude from our analysis those events that, while still accompanied by increased low-level moisture, are not associated with enhanced convective activity over the SW United States (Higgins et al. 2004). However, it would

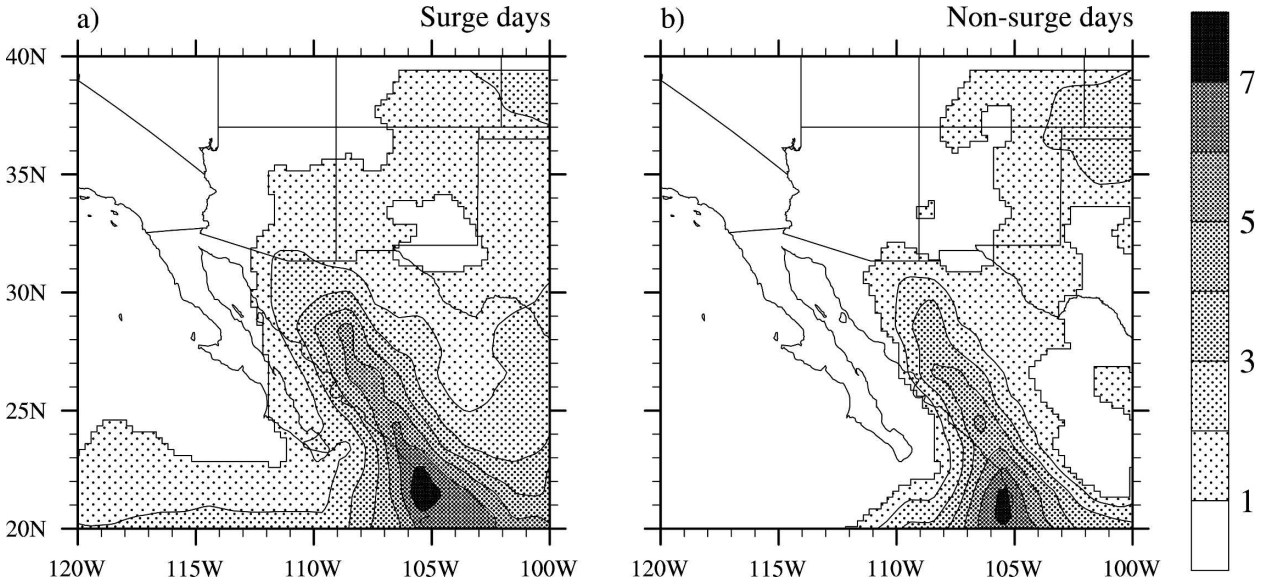

FIG. 10. Mean daily rain rates (mm day^{-1}) for (a) surge and (b) nonsurge days.

TABLE 1. Ratio of the area mean fraction of the total summertime precipitation falling during surge days to the percentage of total summer days that these surge days represent for different thresholds in the surge index used to identify individual surge events in the Sonora, AZ, and NM regions. The fraction of surge days to the total number of summer days (in percent) is shown for each threshold.

Threshold	0.75	0.85	1	1.2	1.4	1.6	2
Days (%)	46	40	36	30	21	15	10
Sonora	1.6	1.6	1.7	1.8	2.3	2.5	3.2
AZ	1.5	1.5	1.5	1.5	1.8	1.9	2.2
NM	1.3	1.3	1.4	1.3	1.3	1.3	1.2

not significantly modify our results, which show a robust relationship between gulf surges and precipitation over the marginal NAM region, providing support to our early hypothesis on the importance of this type of transient activity in the definition of the northward extent of the monsoonal rains.

5. Surges and easterly waves

The regression maps in Figs. 4 and 8 show evidence of northwestward propagation of the wind and precipitation anomalies over Mexico and the SW United States in association with gulf surge events, thus suggesting a relationship between this type of transient and westward-propagating tropical disturbances, such as easterly waves and/or tropical cyclones, in agreement with previous observational and modeling studies. Among them, Stensrud et al. (1997) showed that a mesoscale numerical model could reproduce the occurrence, structure, and propagation characteristics of gulf surges. More importantly, they found that a strong surge is initiated in the model when the passage of an easterly wave trough across western Mexico is preceded by several days by the passage of a midlatitude westerly wave across the western United States. These results were extended in the observational works by Fuller and Stensrud (2000) and Higgins et al. (2004), who explored the relationship between surges (as defined by surface observations at Yuma) and tropical easterly and midlatitude waves over 14- and 30-yr periods, respectively. To explore the possible interplay between tropical easterly and midlatitude westerly waves, we use the procedure developed by Fuller and Stensrud (2000): the easterly (westerly) waves are identified using 700- (200-) hPa meridional winds from the NCEP–NCAR reanalysis. The 700-hPa level appears to be the most suitable for easterly wave identification, because it is low enough in the atmosphere to capture the wave signals, yet high enough to minimize problems associated with the interactions of the waves with the topography in western Mexico. These tropical traveling waves are the same disturbances that later in the year support tropical cyclogenesis in the tropical eastern Pacific and for this reason, in contrast to other studies (Anderson et al. 2000; Douglas and Leal 2003), we do not consider them as a surge initiation mechanism distinct from tropical storms and hurricanes.

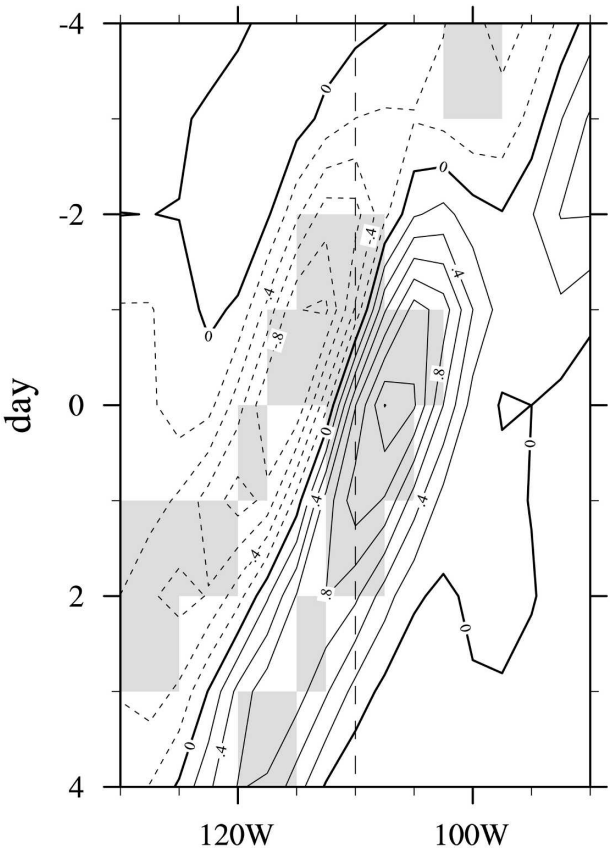

FIG. 11. Lon–time section of lagged regressions of the 700-hPa meridional winds ($m\,s^{-1}$) on the gulf surge index at 20°N. The contour interval is 0.2 $m\,s^{-1}$. Negative anomalies are dashed and the zero line thickened. The dashed vertical line indicates the longitude of the eastern coast of the GoC.

The temporal relationship between the easterly waves and gulf surges is explored by constructing longitude–time Hovmöller diagrams of the 700-hPa meridional winds at 20°N, in which as the easterly waves shift westward across a given longitude, the passage of the wave trough appears as a coherent transition from northerly to southerly winds. The Hovmöller analysis of the lagged regressions of the meridional NCEP–NCAR winds onto the surge index, shown in Fig. 11, reveals a striking association between the onset of a surge (at day 0) and the passage of an easterly wave to the south of the GoC. While variability between individual events is large and remains to be considered, the

results shown here, which represent the most preferred patterns of surge events, suggest that a significant fraction of surges are indeed related to the passage of a tropical easterly wave. The typical frequency of wave trough passages over western Mexico, averaging a little over three per month, as estimated by Fuller and Stensrud (2000), agrees well with our estimated frequency of gulf surge occurrence.

Figures 4 and 8 allow us to trace the patterns of the wind variability over the GoC associated with surge events to the eastern Pacific ITCZ, where they appear to be connected with periods of anomalous westerlies at approximately day −3. Such features are reminiscent of periods of enhanced convection studied during the recent East Pacific Investigations of Climate project (EPIC2001; Raymond et al. 2004), which have been shown to coincide with periods of anomalous westerly flow at 850 hPa. As shown in the analysis of Raymond et al. (2006), during these events the 850-hPa anomalous westerly winds are in geostrophic balance with the lower free-tropospheric pressure to the north caused by the passage of tropical traveling disturbances. This pressure gradient in turn reinforces the pressure gradient associated with the SST distribution, causing enhanced surface southerlies to extend farther to the north and supporting enhanced deep convection in the ITCZ. To explore further this idea, we regress onto the gulf surge index the 850-hPa zonal NCEP–NCAR winds and 10-m meridional QuikSCAT winds in a 4° × 4° box centered at 10°N, 95°W. The box for this analysis has been chosen so as to coincide with the main EPIC2001 study region. The time evolution of the zonal and meridional wind anomalies averaged over the chosen box, shown in Fig. 12, reveals that the days preceding the onset of a surge event are characterized by bursts of westerly winds in the 850-hPa flow over the tropical northeast Pacific region, with anomalies maximizing at day 3 before the onset. The changes in the zonal winds at this level are closely tracked by changes in the surface meridional flow, which features weak but significant positive southerly anomalies. The similarities between the results presented in Raymond et al. (2006), which pertain to episodes of enhanced convection over the tropical Pacific, and the results presented here, which specifically relate to the occurrence of gulf surge events, therefore suggest that gulf surges represent the "mesoscale" manifestation over the GoC of the larger-scale tropical disturbances that control the synoptic-scale variability in the eastern Pacific ITCZ.

While the connection between gulf surges and tropical waves appears remarkable in our analysis, a clear relationship between surge events and eastward-propagating midlatitude waves fails to emerge from the Hovmöller diagrams of lagged regressions of 200-hPa meridional winds at 40°N. However, in agreement with Higgins et al. (2004), there appears to be an association with quasi-stationary features such as the position of the upper-tropospheric monsoon anticyclone that requires further investigation. The importance of the location of the upper-tropospheric monsoon ridge in determining bursts and breaks within a monsoon season has been highlighted by several authors (Carleton et al. 1990; Watson et al. 1994). A southwestern displacement of the upper-level anticyclone over northwestern Mexico places the SW United States under the drying influence of the westerlies, thus promoting break conditions, whereas a northeasterly shift of the monsoon high is associated with increased flow of moisture from the south, thus being more conducive to bursts of convective activity. In a recent study, Kiladis and McKim (2004) have argued that ridging over the midwestern United States, which is often observed in connection with intraseasonal precipitation events over Arizona and New Mexico during the summer monsoon, is tied to the dispersion of Rossby waves from the North Pacific into North America, which, by inducing changes in the circulation patterns, produce anomalous southerly flow and moisture advection over the region. These results, together with our findings, suggest that the complex interactions between synoptic and mesoscale circulations, which are the fundamental processes responsible of the temporal and spatial variability of the monsoon, may ultimately be related to midlatitude and tropical wave activity. While the easterly waves provide the necessary low-level moisture inflow into the SW United States by triggering gulf surges, wave energy originating from midlatitudes creates the large-scale environment more conducive to thunderstorm development by displacing the monsoon high. Although not as initially en-

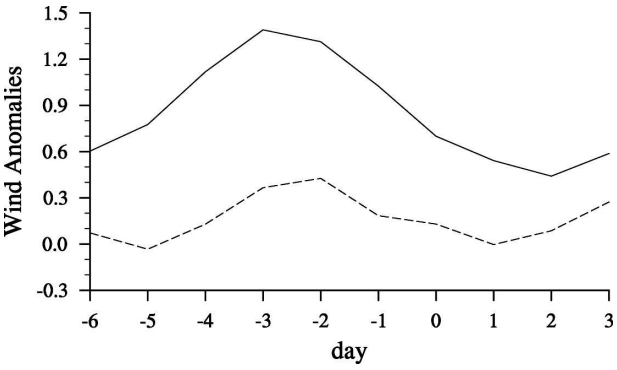

FIG. 12. Lagged regression vs time of 850-hPa zonal NCEP–NCAR (solid) and 10 m meridional QuikSCAT (dashed) winds averaged over a 4° × 4° box centered at 10°N, 95°W in the eastern Pacific ITCZ.

visioned by Stensrud et al. (1997), the interaction between the Tropics and midlatitudes may yet play a role in determining the basic structure of the NAM.

6. Discussion

a. NCEP–ERA-40 comparison

All the results shown in the previous sections are based on the NCEP–NCAR reanalysis. In this section, we address the question as to how different the results are when we use the ERA-40 reanalysis. Because of the higher resolution of the global model underlying them, the ERA-40 data provide a better representation of the state of the lower troposphere over the NAM region, in particular over the GoC. It is therefore reasonable to expect that the regression maps based on this dataset will reveal smaller-scale features of the gulf surge phenomenon that the NCEP–NCAR data are not capable of capturing. Keeping in mind that ERA-40 provides data only up to August 2002, the results discussed in this section specifically pertain to the four summers (1999–2002) for which both reanalyses are available.

In general, the spatial patterns of the NCEP–NCAR-based horizontal regressions are in good agreement with the ERA-40-based ones, which confirms that, despite its deficiencies, the former is a very valuable product for our regression analysis and justifies its extensive use in this study. The ERA-40 however better captures localized features, such as the high pressure and cold temperature tongue (see Figs. 4 and 5 at days 0–2), that develop along the GoC in association with a gulf surge. This results in larger anomalies (up to ~20%) and stronger zonal gradients over the GoC and the surrounding regions in all of the ERA-40 anomalous fields. The specific humidity, which shows significant differences between the ERA-40 and NCEP–NCAR reanalyses, deserves a separate discussion.

Lagged regressions of the ERA-40 925-hPa specific humidity onto the gulf surge index, to be compared with the NCEP–NCAR-based Fig. 6, are shown in Fig. 13.[2] Consistently but much more pronouncedly than in other fields, the ERA-40 humidity anomalies are stronger than the NCEP–NCAR ones: note that in Fig. 13 the contour spacing is twice that in Fig. 6. Small-scale localized features that are evident in Fig. 13 but absent in Fig. 6, such as the local minimum and maximum in the specific humidity anomalies along the GoC at day 0, may be influenced by sounding station data at Guaymas and Mazatlan. At early lags (day −3), the spatial structure of the anomalies is particularly different, with the NCEP–NCAR data showing drier-than-normal conditions over the entire analysis domain and the ERA-40 data showing evidence of weak but positive anomalies to the south of the GoC, near 18°N. At later times, the two reanalyses tend to better agree—for instance, they locate the zero contour at around the same latitude over the GoC—but important discrepancies remain. The most notable one is the extent to which the ERA-40 specific humidity "feels" the presence of the Sierra Madre Occidental range on the west coast of mainland Mexico. This is clearly evident starting from day −1 in the packing and closing off of the positive anomaly contours on the eastern coast of the GoC, just over the western flank of the mountain range. No such feature appears in the NCEP–NCAR regressions. This is more than just a curiosity: it provides evidence that, while positive humidity and precipitation anomalies originating from the Gulf of Mexico are found on the east coast of Mexico during gulf surge events (Fig. 8), the bulk of low-level moisture being advected into the marginal monsoon regions has its origin in the tropical Pacific and the GoC. Mixing between moisture from the two sources appears to be effectively prevented at low levels by the presence of the elevated topography. As suggested by the empirical study by Schmitz and Mullen (1996), mixing induced by the convection over the Sierra Madre Occidental can still occur, but only at mid- and upper levels.

Finally, the average vertical structure of gulf surges emerging from the ERA-40 vertical cross sections of the alongshore wind, specific humidity, and air temperature is in good agreement with the NCEP–NCAR-based one discussed at the end of section 3. More specifically, the ERA-40 data confirm that field anomalies associated with surge events are not confined to the lower troposphere, but extend to higher levels. This appears to be particularly true for the alongshore winds, whose positive anomalies over the GoC feature an equivalent-barotropic structure that stretches beyond 8 km.

b. Comparison with other gulf surge indices

With several gulf surge definitions and identification methods already existing in the literature, it is natural to ask how the gulf surge index introduced in this study differs from and compares with others, the most widely used being based on hourly surface observations at Yuma, Arizona, located at the northern mouth of the GoC (Fuller and Stensrud 2000; Higgins et al. 2004). Gulf surge indices based on Yuma observations—or

[2] We do not show the NCEP–NCAR regressions for the time span 1999–2002 during which the ERA-40 data are available, as they not differ significantly from the ones shown in Fig. 6

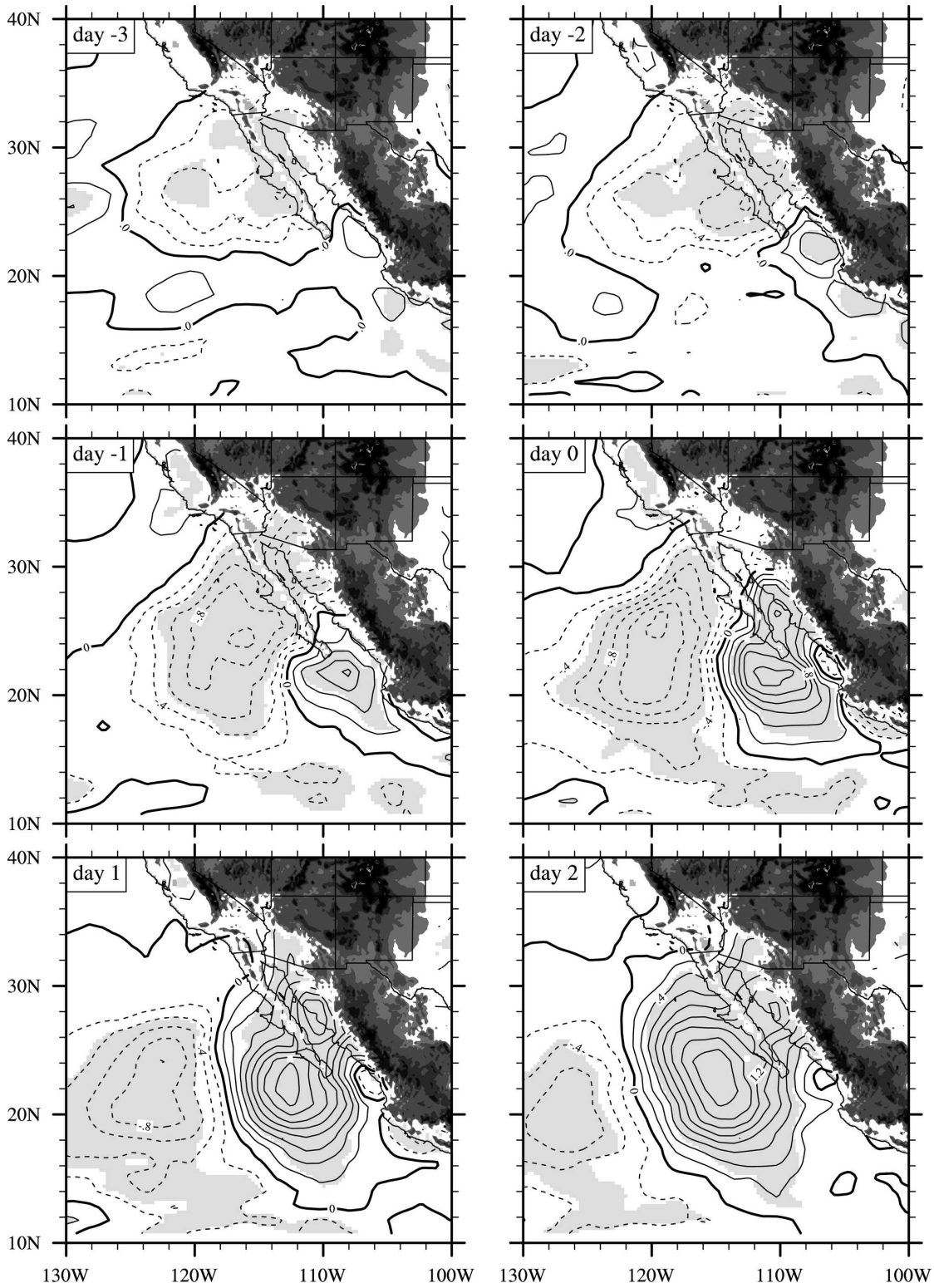

FIG. 13. Lagged regressions from day −3 to day +2 of the ERA-40 925-hPa specific humidity onto the leading PC. The contour interval is 0.2 g kg^{-1}. Negative anomalies are dashed and the zero line thickened. Shading indicates regions where anomalies are statistically significant at the 95% level. Areas with topography (in grayscale contours) above the 925-hPa level have been masked out.

more generally on observations collected at one single station—have the advantage of providing longtime records spanning more than two decades and surge identification criteria readily applicable in an operational context, but suffer from several shortcomings. First, by using only surface data at one single station some surges may be not identified, since surges do not always propagate into Arizona. Second, outflow from isolated thunderstorms, while lasting only a few hours, can show the same characteristics as surges. Finally, for a surge to be identified, several days of relatively lower dewpoint temperatures must be observed at Yuma prior to the surge: if dewpoint temperatures remain elevated throughout a longer time period, it is impossible to distinguish any surge event, since an increase in the dewpoint temperature value is the most distinguishable characteristic of a surge as it arrives at Yuma. Although temporally limited to the latest six summers, our index, being based on the dynamical environment associated with these transients, does not suffer from any of these ambiguities. A comparison of four summers (1999–2002) of Yuma data with our index shows that, while the agreement between the two indices is generally good, the source of the largest discrepancies is indeed the existence in the Yuma data of extended periods of elevated dewpoint temperatures. These tend to occur in late July and August, can last up to a few weeks, and are shown by our index, which does not feature such prolonged periods of elevated values, to be sustained by the occurrence of distinct episodes.

Surge events that our index is not capable of identifying and that are therefore not included in our analysis are those that originate in the central part of the GoC and remain confined over its northern half. While defined as "minor" because of their more limited spatial extent, these surges are believed to have similar effects on the monsoonal precipitation to major surges affecting the entire GoC (Adams and Comrie 1997), which suggests that consideration of these events would result in even higher percentages of the total summertime rainfall over the SW United States during surge days than the ones shown in Fig. 9. Although not through the leading PC, our EOF analysis of the summertime alongshore winds may still prove useful in the identification of these minor episodes. For instance, the third EOF, which accounts for no more than ~8% of the total variance, appears to be capable of capturing changes in the low-level winds that are confined to the north of the Midriff Islands. While promising, this issue requires further study.

It could be argued that our index is also unable to detect those surge events that, while traveling along the entire GoC, do not extend across its entire longitudinal span. While this is a valid concern, we find that the statistically significant and well-separated EOFs as per the criterion of North et al. (1982), which together explain more than 90% of the the summertime GoC wind variance, all show longitudinally coherent wind anomalies. This suggests that, albeit possible, surges with a short spatial extent across the GoC are a relatively rare occurrence.

7. Summary

An EOF analysis of the daily JJAS QuikSCAT alongshore winds for six summers has been used to determine the leading mode of synoptic-scale variability of the GoC low-level flow during the NAM season. A gulf surge mode, characterized by anomalous southerly flow along the GoC, emerges from this analysis as the leading EOF, thus confirming the view of gulf surges as a dynamical mode distinct from the background flow and motivating our interpretation of the associated principal component time series as an objective index for gulf surge occurrence.

Lagged regressions of QuikSCAT, NCEP–NCAR, and ERA-40 fields onto this index reveal that gulf surges are usually associated with a low-level, northwestward-moving cyclonic anomaly, which, located at the onset to the southwest of the tip of Baja California, provides anomalous southeasterly flow into the GoC to its eastern flank. A high pressure and cold temperature tongue, confined over the gulf, and positive specific humidity anomalies, spanning from the tropical Pacific to the western flanks of the Sierra Madre Occidental, accompany the development of the southerly winds. Along the GoC, all the anomalies show a deep equivalent barotropic structure extending several kilometers from the surface. The anomalous low-level moisture transport provided by gulf surges appears to strongly influence the monsoonal precipitation patterns, especially over the coastal plains on the eastern boundary of the GoC and Arizona. In these regions, the surge index explains a fraction of the total summertime precipitation that exceeds 70%. Additionally, rain rates computed for surge and nonsurge days show that the mean daily precipitation falling in these areas during nonsurge days is almost negligible, being less than 1 mm day^{-1}. Although traditionally considered mesoscale features confined along the GoC, gulf surges are shown to be intimately tied to large-scale tropical disturbances, such as easterly waves and/or tropical cyclones. The connection between gulf surges and tropical disturbances has been recognized and explored by a number of previous studies (Anderson et al. 2000; Stensrud et al. 1997; Fuller and Stensrud 2000; Douglas and Leal

2003; Higgins et al. 2004). The most novel aspect in our analysis relies on our use of a global precipitation product, which provides data over the oceans, as well as over land, and allows us to trace the patterns of precipitation variability associated with gulf surges to periods of enhanced convection and anomalous westerlies over the eastern Pacific ITCZ. Not only does this provide further evidence of the influence of tropical processes on the initiation of gulf surges, but it also confirms the importance of the tropical Pacific/GoC as the dominant low-level moisture source for the NAM.

The results summarized above, in addition to providing a detailed description of gulf surge events and their relationship with the monsoonal precipitation, highlight the role that this type of transient plays in shaping important features of the NAM, such as the northward extent of its rains. Indeed, the picture of the NAM as an envelope of transient activity is one of the most fascinating aspects to emerge from our analysis, further raising the question as to how different the monsoon would be were transients absent.

As already mentioned in the introduction, our incomplete understanding of many aspects of the NAM stems from the lack, until recent times, of observational data in the region. The high spatial and temporal resolution products (such as QuikSCAT and the ERA-40 used in this study), which have recently become available, are proving capable of providing new insights into the monsoon structure and variability. Used in conjunction with the enhanced observations collected during the North American Monsoon Experiment in summer 2004, these products will help us elucidate further the relationship between gulf surges and precipitation, as well as the relevant dynamical processes controlling gulf surges.

Acknowledgments. The QuikSCAT level 3 ocean wind vector data were obtained from the Physical Oceanography Distributed Active Archive Center (PODAAC) at NASA JPL in Pasadena, California (information online at http:/podaac.jpl.nasa.gov). The blended global GPCP 1DD product was provided by the NASA Goddard Space Flight Center's Laboratory for Atmospheres (ftp://rsd.gsfc.nasa.gov/pub/1dd), which develops and computes the 1DD as a contribution to the GEWEX GPCP. The ECMWF ERA-40 data were obtained from the data system section at NCAR. The NCEP–NCAR renalaysis data are provided by the NOAA–CIRES Climate Diagnostics Center, Boulder, Colorado, via their Web site (http://www.cdc.noaa.gov). The authors thank Dennis Shea for his help with the satellite products, Roger Wakimoto for motivating interest in the monsoon, George Kiladis for discussions during the early stages of this work, and Tapio Schneider for helpful comments and suggestions through the course of this study. Comments by Mike Douglas and one anonymous reviewer helped improve this manuscript. This work was supported by NASA through Fellowship NGT530499 and Grant NAG512559.

REFERENCES

Adams, D. K., and A. C. Comrie, 1997: The North American monsoon. *Bull. Amer. Meteor. Soc.,* **78,** 2197–2213.

Anderson, B. T., J. O. Roads, and S. C. Chen, 2000: Large scale forcing of summertime monsoon surges over the Gulf of California to the southwestern United States. *J. Geophys. Res.,* **105,** 24 455–24 468.

Berbery, E. H., 2001: Mesoscale moisture analysis of the North American monsoon. *J. Climate,* **14,** 121–137.

——, and M. S. Fox-Rabinovitz, 2003: Multiscale diagnosis of the North American monsoon system using a variable-resolution GCM. *J. Climate,* **16,** 1929–1947.

Bordoni, S., P. E. Ciesielski, R. H. J. B. D. McNoldy, and B. Stevens, 2004: The low-level circulation of the North American monsoon as revealed by QuikSCAT. *Geophys. Res. Lett.,* **31,** L10109, doi:10.1029/2004GL020009.

Bourassa, M. A., D. Legler, J. J. O'Brien, and S. R. Smith, 2003: SeaWinds validation with research vessels. *J. Geophys. Res.,* **108,** 3019, doi:10.1029/2001JC001028.

Bryson, R., and W. P. Lowry, 1955: Synoptic climatology of the Arizona summer precipitation singularity. *Bull. Amer. Meteor. Soc.,* **36,** 329–339.

Carleton, A. M., D. A. Carpenter, and P. J. Weber, 1990: Mechanisms of interannual variability of the southwest United States summer rainfall. *J. Climate,* **3,** 999–1015.

Douglas, M. W., and J. C. Leal, 2003: Summertime surges over the Gulf of California: Aspects of their climatology, mean structure, and evolution from radiosonde, NCEP reanalysis, and rainfall data. *Wea. Forecasting,* **18,** 55–74.

——, R. A. Maddox, K. Howard, and S. Reyes, 1993: The Mexican monsoon. *J. Climate,* **6,** 1665–1677.

Ebuchi, N., H. C. Graber, and M. J. Caruso, 2002: Evaluation of wind vectors observed by QuikSCAT/SeaWinds using ocean buoy data. *J. Atmos. Oceanic Technol.,* **19,** 2049–2062.

Fuller, R. D., and D. J. Stensrud, 2000: The relationship between tropical easterly waves and surges over the Gulf of California during the North American monsoon. *Mon. Wea. Rev.,* **128,** 2983–2989.

Gochis, D. J., A. Jimenez, C. J. Watts, J. G. Garatuza-Payan, and W. J. Shuttleworth, 2004: Analysis of 2002 and 2003 warm-season precipitation from the North American Monsoon Experiment event rain gauge network. *Mon. Wea. Rev.,* **132,** 2938–2953.

Green, C. R., and W. D. Sellers, 1964: *Arizona Climate.* University of Arizona Press, 503 pp.

Hales, J. E., 1972: Surges of maritime tropical air northward over the Gulf of California. *Mon. Wea. Rev.,* **100,** 298–306.

Hastings, R. J., and R. Turner, 1965: Seasonal precipitation regime in Baja California. *Geogr. Ann.,* **47A,** 204–223.

Higgins, R. W., and W. Shi, 2001: Intercomparison of the principal modes of interannual and intraseasonal variability of the North American monsoon system. *J. Climate,* **14,** 403–417.

——, ——, and C. Hain, 2004: Relationships between Gulf of

California moisture surges and precipitation in the southwestern United States. *J. Climate,* **17,** 2983–2997.

Huffman, G. J., R. F. Adler, M. M. Morrissey, D. T. Bolvin, S. Curtis, R. Joyce, B. McGavock, and J. Susskind, 2001: Global precipitation at one-degree daily resolution from multisatellite observations. *J. Hydrometeor.,* **2,** 36–50.

Kaihatu, J. M., R. A. Handler, G. O. Marmorino, and L. K. Shay, 1998: Empirical orthogonal function analysis of ocean surface currents using complex and real-vector methods. *J. Atmos. Oceanic Technol.,* **15,** 927–941.

Kalnay, E., and Coauthors, 1996: The NCEP/NCAR 40-Year Reanalysis Project. *Bull. Amer. Meteor. Soc.,* **77,** 437–471.

Kiladis, G. N., and E. McKim, 2004: Intraseasonal modulation of precipitation over the North American monsoon region. Preprints, *15th Symp. on Global Change and Climate Variations,* Seattle, WA, Amer. Meteor. Soc., CD-ROM, 11.4.

Livezey, R. E., and W. Y. Chen, 1983: Statistical field significance and its determination by Monte Carlo techniques. *Mon. Wea. Rev.,* **111,** 46–59.

Meitin, J. G., K. W. Howard, and R. Maddox, 1991: The South-West Area Monsoon Project: Daily operations summary. National Severe Storm Laboratory Tech. Rep., 115 pp.

Mitchell, D. L., D. Ivanova, R. Rabin, T. J. Brown, and K. Redmond, 2002: Gulf of California sea surface temperatures and the North American monsoon: Mechanistic implications from observation. *J. Climate,* **15,** 2261–2281.

North, G. R., T. L. Bell, R. F. Cahalan, and F. J. Moeng, 1982: Sampling errors in the estimation of empirical orthogonal functions. *Mon. Wea. Rev.,* **110,** 699–706.

Pickett, M. H., W. Tang, L. Rosenfeld, and C. Wash, 2003: QuikSCAT satellite comparisons with nearshore buoy data off the U.S. west coast. *J. Atmos. Oceanic Technol.,* **20,** 1869–1879.

Raymond, D. J., and Coauthors, 2004: EPIC2001 and the coupled ocean–atmosphere system of the tropical east Pacific. *Bull. Amer. Meteor. Soc.,* **85,** 1341–1354.

——, C. Bretherton, and J. Molinari, 2006: Dynamics of the intertropical convergence zone of the East Pacific. *J. Atmos. Sci.,* **63,** 582–597.

Reitan, C. H., 1957: The role of precipitable water vapor in Arizona summer rains. Tech. Rep. on the Meteorology and Climatology of Arid Regions 2, Institute of Atmospheric Physics, The University of Arizona, Tucson, AZ, 19 pp.

Schlax, M. G., D. B. Chelton, and M. F. Freilich, 2001: Sampling errors in wind fields constructed from single and tandem scatterometer datasets. *J. Atmos. Oceanic Technol.,* **18,** 1014–1036.

Schmitz, J. T., and S. L. Mullen, 1996: Water vapor transport associated with the summertime North American monsoon as depicted by ECMWF analyses. *J. Climate,* **9,** 1621–1634.

Stensrud, D. J., R. L. Gall, S. L. Mullen, and K. W. Howard, 1995: Model climatology of the Mexican monsoon. *J. Climate,* **8,** 1775–1794.

——, ——, and M. K. Nordquist, 1997: Surges over the Gulf of California during the Mexican monsoon. *Mon. Wea. Rev.,* **125,** 417–437.

Uppala, S. M., and Coauthors, 2005: The ERA-40 reanalysis. *Quart. J. Roy. Meteor. Soc.,* **131,** 2961–3012.

Watson, A. W., R. E. Lopez, and R. L. Holle, 1994: Diurnal cloud-to-ground lightning patterns in Arizona during the southwest monsoon. *Mon. Wea. Rev.,* **122,** 1716–1725.

Yu, B., and J. M. Wallace, 2000: The principal modes of interannual variability of the North American monsoon system. *J. Climate,* **13,** 2794–2800.